

https://dspace.org/

A Study To Optimize Ore Evaluation At Western Deep Levels Gold Mine, Witwatersrand, By Using Geostatistics And Geological Subdivision

Braun, Rolf

2015-01-12
http://hdl.handle.net/10539/16439

Downloaded from a DSpace repository. https://dspace.org/

A STUDY TO OPTIMIZE ORE EVALUATION AT WESTERN DEEP LEVELS GOLD MINE, WITWATERSRAND, BY USING GEOSTATISTICS AND GEOLOGICAL SUBDIVISION

Rolf Braun

A thesis submitted to the Faculty of Engineering, University of the Witwatersrand, Johannesburg, in fulfilment of the requirements for the degree of Doctor of Philosophy in Mining Engineering

Johannesburg 1988

DECLARATION

The work presented in this thesis is my own and has not been submitted for a degree at any other university.

.....

(Rolf Braun)

September 1988

ABSTRACT

The auriferous Carbon Leader reef on the Western Deep Levels gold mine which is the subject of this study can be subdivided into two types of sedimentological units, each with its characteristic spatial variability.

The potential advantage to be gained from the use of this information as well as the introduction of various geostatistical techniques is examined in relation to the present system of estimation of ore reserves on the mine.

For longwall mining as practised on the mine kriging provides a significant benefit over the present method and the further improvement gained by subdivision is assessed as follows:

- while the conditional unbiasedness of the estimates is not affected by subdivision, the actual error variances of the block estimates are reduced.
-the kriging estimation variance obtained from the geostatistical model only becomes a valid estimate of the actual error distribution, if the Carbon Leader reef is subdivided. This is so because subdivision provides acceptable stationarity of the semivariogram.

Simple kriging is the only method that gives conditionally unbiased estimates, the difference between untransformed and logtransformed kriging is negligible.

ACKNOWLEDGEMENTS

The work described in this thesis forms part of the research programme of the Chamber of Mines of South Africa. The author wishes to thank the Chamber of Mines for their financial support, and gratefully acknowledges the permission of Western Deep Levels gold mine to submit this thesis.

The author is greatly indebted to Professor D.G. Krige for his advice, guidance and constant encouragement over the course of this study.

He also wishes to especially thank the following people:

- Dr. M. Nami and Mr. L. Verrezen (Chamber of Mines) for the many fruitful discussions on sedimentology.

- Mrs. I. Dohm and Mr. H. Elliot (Western Deep Levels gold mine) for familiarizing the author with the problems and limitations encountered in practice.

- Mr. R. Fong (University of the Witwatersrand) for his advice on computer programming problems.

CONTENTS

DECLARATION I
ABSTRACT II
ACKNOWLEDGEMENTS III
CONTENTS IV
LIST OF FIGURES VII
LIST OF TABLES XII
LIST OF SYMBOLS XIII
PREFACE XVI

1 INTRODUCTION 1
1.1 General 1
1.2 Outline 3
1.3 Geographical and geological setting of the study area 5

2 PREVIOUS INVESTIGATIONS IN THE RELATION OF GOLD DISTRIBUTION AND SEDIMENTOLOGY IN THE CARBON LEADER REEF 9
2.1 Description of sedimentology 9
2.2 Interpretation of sedimentology 11

3 SEDIMENTOLOGICAL STUDY 13
3.1 Method 13
3.2 Practical limitations 17
3.3 Description of Carbon Leader reef in the study area 18
3.4 Classification of sedimentary characteristics 23
3.5 Interpretation of sedimentology 24
3.6 Facies distribution in study area 29
3.6.1 Comparison of geological data and sampling data 29
3.6.2 Facies map 35

4 GEOSTATISTICAL STUDY 38
4.1 Present mine valuation technique 38
4.2 Comparison of different estimation techniques 42
4.3 Comparison of mine estimates with true data 46

4.4 Assay data 52
4.41 Collection 52
4.42 Analysis 53
4.5 Geostatistical estimation of mine ore blocks without subdivision. 64
4.5.1 Regularisation of sample data and analysis of regularized data 64
4.5.2 Ore reserve estimation 71
4.5.3 Analysis of simulation 76
4.6 Subdivision of study area 82
4.6.1 Basic considerations 82
4.6.2 Geostatistical characteristics of the different subfacies 84
4.6.3 Individual analysis of mineralisation in top and bottom band for Subfacies 1 113
4.7 Simulation of ore reserve estimation for mine blocks, with and without subdivision 116
4.7.1 Ore reserve estimation 116
4.7.2 Analysis of results of $(100m)^2$ oreblock estimation in the individual subareas 118
4.7.2.1 Influence of subdivision on grade estimates 119
4.7.2.2 Evaluation of different methods 131
4.7.2.3 Evaluation of different semi-variogram transformations 135
4.7.2.4 Preliminary conclusions 139
4.7.3 Analysis of results of $(100m)^2$ ore-blocks for the combined subareas 141
4.8 Comparison of actual and estimated estimation errors 149

5 POSSIBLE IMPROVEMENTS BASED ON THEORETICAL CALCULATIONS 160
5.1 Ore block size and shape 160
5.1.1 Theoretical considerations towards the optimization of ore block size and shape 160
5.1.2 Practical verification 163

5.2 Theoretical considerations towards the optimization of the sampling grid 167
6 CONCLUSIONS 178

REFERENCES 180

APPENDIX 1: METHODS AND TECHNIQUES USED 184
A1.1 Determination of the minimum number of samples for regularized data blocks and 'true' blocks 185
A1.2 Semivariogram transformations 192

APPENDIX 2: SOFTWARE DEVELOPMENT 195
A2.1 Nimrod 196
A2.2 Digitize 201
A2.3 Convert 203
A2.4 Probplot 204
A2.5 Datablok 207
A2.6 Uksim 209
A2.7 Uktrend 214

LIST OF FIGURES

1.1a	Location of the Carletonville Goldfield in the Witwatersrand	6
1.1b	Mining lease areas of the Carletonville Goldfield	6
1.2	Geological north-south section through the Carletonville Goldfield	8
3.1	Sedimentological logging sheet used for underground mapping	14
3.2	Stratigraphic code for different units	15
3.3	Sudden thickening of bottom conglomerate layer and occurence of shale	19
3.4	Idealized sedimentological section through the conglomerate unit	22
3.5	Schematic block diagram of depositional model	28
3.6	Influence of reef in hangingwall on channel width as recorded during assay sampling	29
3.7	Plot of true channel width against the assaying channel width	34
4.1	Calculation of accumulation in multiple reef band area.	38
4.2	Exponential decreas of row average gold values from north to south	40
4.3	Regression diagram mine method north - eastern quadrant	47
4.4	Regression diagram mine method southern quadrants	51
4.5	Regression diagram for true and simulated mine estimates - southern quadrants	51
4.6	Logarithmic probability plot of 36 160 assay data	54
4.7	Plot of semivariogram ranges in different directions	57
4.8	Directional logtransformed semivariograms of shaft area	60
4.9	Plot of experimental and theoretical block variances, shaft area	61
4.10	Directional Hawkins & Cressie semivariograms shaft area	62
4.11a	N-S untransformed experimental semivariogram and models, shaft area	63
4.11b	E-W untransformed experimental semivariogram and models, shaft area	63
4.12	Logarithmic probability plot of regularized (50m by 50m) data blocks	65
4.13a	N-S logtransformed semivariogram regularized data blocks	67
4.13b	E-W logtransformed semivariogram regularized data blocks	67
4.14a	N-S Hawkins & Cressie semivariogram regularized data blocks	68
4.14b	E-W Hawkins & Cressie semivariogram regualrized data blocks	68
4.15a	N-S untransformed experimental semivariogram and models for data blocks	69

4.15b N-S untransformed experimental semivariogram and models for data blocks 69
4.16a Standard mining situation at time of ore block estimation, and simulated longwall 71
4.16b Estimation set-up used to simulate the longwall mining condition 72
4.17a,b Plot of slope against observed error variance 79
4.18 Plot of average kriging variance against observed error variance 81
4.19 Logarithmic probability plot, subarea S1.1 90
4.20 Logarithmic probability plot, subarea S1.2 91
4.21 Logarithmic probability plot, subarea S2.1 92
4.22 Logarithmic probability plot, subarea S2.2 93
4.23 Logarithmic probability plot, subarea S2.3 94
4.24a N-S logtransformed semivariogram S1.1 95
4.24b E-W logtransformed semivariogram S1.1 95
4.24c N-S Hawkins & Cressie semivariogram S1.1 96
4.24d E-W Hawkins & Cressie semivariogram S1.1 96
4.25 Theoretical and experimental variance - size of area graph S1.1 97
4.26 Theoretical and experimental variance - size of area graph S1.2 97
4.27a N-S logtransformed semivariogram S1.2 98
4.27b E-W logtransformed semivariogram S1.2 98
4.27c N-S Hawkins & Cressie semivariogram S1.2 99
4.27d E-W Hawkins & Cressie semivariogram S1.2 99
4.28a N-S logtransformed semivariogram S2.1 100
4.28b E-W logtransformed semivariogram S2.1 100
4.28c Omindirectional logtransformed semivariogram S2.1 101
4.28d Omnidirectional Hawkins & Cressie semivariogram S2.1 101
4.29 Theoretical and experimental variance - size of area graph S2.1 102
4.30a N-S logtransformed semivariogram S2.2 103
4.30b E-W logtransformed semivariogram S2.2 103
4.30c NE-SW logtransformed semivariogram S2.2 104
4.30d NW-SE logtransformed semivariogram S2.2 104
4.30e Omindirectional logtransformed semivariogram S2.2 105
4.30f Omnidirectional Hawkins & Cressie semivariogram S2.2 105
4.31 Theoretical and experimental variance - size of area graph S2.2 106
4.32a N-S logtransformed semivariogram S2.3 107
4.32b E-W logtransformed semivariogram S2.3 107
4.32c Omindirectional logtransformed semivariogram S2.3 108
4.32d Omnidirectional Hawkins & Cressie semivariogram S2.3 108
4.33 Theoretical and experimental variance - size of area graph S2.3 109
4.34a Logtransformed semivariogram models 110
4.34b Backtransformed semivariogram models 111
4.34c Hawkins & Cressie semivariogram models 112
4.35a Directional logtransformed semivariograms subfacies 1 reef type 1 115
4.35b Directional logtransformed semivariograms subfacies 1 reef type 2 115

4.36a Plot of mean error of kriging methods vs number of pairs - overall semivariogram 120
4.36b Plot of mean error of kriging methods vs number of pairs - local semivariograms 120
4.37a Plot of slope vs actual error variance, S1.1, overall semivariogram 121
4.37b Plot of slope vs actual error variance, S1.1, local semivariogram 121
4.38a Plot of slope vs actual error variance, S1.2, overall semivariogram 122
4.38b Plot of slope vs actual error variance, S1.2, local semivariogram 122
4.39a Plot of slope vs actual error variance, S2.1, overall semivariogram 123
4.39b Plot of slope vs actual error variance, S2.1, local semivariogram 123
4.40a Plot of slope vs actual error variance, S2.2, overall semivariogram 124
4.40b Plot of slope vs actual error variance, S2.2, local semivariogram 124
4.41a Regression diagram, mine method (100m*100m) shaft area 146
4.41b Regression diagram, regressed mine estimates, (100m*100m), shaft area 146
4.41c Regression diagram, simple lognormal kriging, - without subdivision (100m*100m), shaft area 147
4.41d Regression diagram, simple lognormal kriging, - with subdivision (100m*100m), shaft area 147
4.42a Regression diagram, simple kriging - without subdivision,(100m*100m), shaft area 148
4.42b Regression diagram, simple kriging - with subdivision, (100m*100m), shaft area 148
4.43a Actual and estimated error distribution, simple lognormal kriging, S1.1 150
4.43b Actual and estimated error distribution, simple kriging, S1.1 150
4.44a Actual and estimated error distribution, simple lognormal kriging, S1.2 151
4.44b Actual and estimated error distribution, simple kriging, S1.2 151
4.45a Actual and estimated error distribution, simple lognormal kriging, S2.1 152
4.45b Actual and estimated error distribution, simple kriging, S2.1 152
4.46a Actual and estimated error distribution, simple lognormal kriging, S2.2 153
4.46b Actual and estimated error distribution, simple kriging, S2.2 153
4.47a Plot of actual error vs estimated error, simple lognormal kriging, S1.1 156
4.47b Plot of actual error vs estimated error, simple kriging, S1.1 156
4.48a Plot of actual error vs estimated error, simple lognormal kriging, S1.2 157
4.48b Plot of actual error vs estimated error, simple kriging, S1.2 157
4.49a Plot of actual error vs estimated error, simple lognormal kriging, S2.1 158

4.49b Plot of actual error vs estimated error, simple kriging, S2.1 158
4.50a Plot of actual error vs estimated error, simple lognormal kriging, S2.2 159
4.50b Plot of actual error vs estimated error, simple kriging, S2.2 159
5.1 Subdivision of (100m*100m) ore block into sub-blocks 161
5.2 Estimation setup for kriging of (200m*50m) ore blocks 163
5.3a Regression diagram (200m*50m) ore blocks, simple lognormal kriging, shaft area 166
5.3b Regression diagram (200m*50m) ore blocks, simple kriging, shaft area 166
5.4a Error variance of (200m*50m) ore block, depending on sample grid, simple lognormal kriging, S1.1 169
5.4b Error variance of (200m*50m) ore block, depending on sample grid, simple kriging, S1.1 169
5.4c Error variance of (200m*50m) ore block, depending on sample grid, simple lognormal kriging, S1.2 170
5.4d Error variance of (200m*50m) ore block, depending on sample grid, simple kriging, S1.2 170
5.4e Error variance of (200m*50m) ore block, depending on sample grid, simple lognormal kriging, S2.1 171
5.4f Error variance of (200m*50m) ore block, depending on sample grid, simple kriging, S2.1 171
5.4g Error variance of (200m*50m) ore block, depending on sample grid, simple lognormal kriging, S2.1 172
5.4h Error variance of (200m*50m) ore block, depending on sample grid, simple kriging, S2.1 172
5.5 Number of samples required per (200m*50m) area, depending on sample grid 173
5.6a Plot of logarithmic estimation variance of (200m*50m) ore block vs distance of nearest sampled face to ore block 176
5.6b Plot of estimation variance of (200m*50m) ore block vs distance of nearest sampled face to ore block 176
A1.1 Plot of logarithmic block variance vs number of samples in block, (50m*50m) blocks, shaft area 189
A1.2 Plot of logarithmic block variance vs number of samples in block, (100m*100m) blocks, shaft area 189
A1.3 Plot of logarithmic block variance vs number of samples in block, (100m*100m) blocks, S1.1 190
A1.4 Plot of logarithmic block variance vs number of samples in block, (100m*100m) blocks, S1.2 190

A1.5 Plot of logarithmic block variance vs number of samples in block, (100m*100m) blocks. S2.1 191
A1.6 Plot of logarithmic block variance vs number of samples in block, (100m*100m) blocks, S2.2 191

LIST OF TABLES

3.1	Reef type characteristics	23
3.2	Correlation of channel width as recorded by geologists and samplers	31
4.1	Shaft area, regression analysis of 305 (100m*100m) ore blocks	80
4.2	Basic statistics of five subpopulations	84
4.3	Comparison of semivariograms of subfacies	88
4.4	Weight given to mean in case of simple kriging	125
4.5a	S1.1, regression analysis of 10 (100m*100m) ore blocks, overall semivariogram	126
4.5b	S1.1, regression analysis of 10 (100m*100m) ore blocks, local semivariogram	126
4.6a	S1.2, regression analysis of 34 (100m*100m) ore blocks, overall semivariogram	127
4.6b	S1.2, regression analysis of 34 (100m*100m) ore blocks, local semivariogram	127
4.7a	S2.1, regression analysis of 82 (100m*100m) ore blocks, overall semivariogram	128
4.7b	S2.1, regression analysis of 82 (100m*100m) ore blocks, local semivariogram	128
4.8a	S2.2, regression analysis of 37 (100m*100m) ore blocks, overall semivariogram	129
4.8a	S2.2, regression analysis of 37 (100m*100m) ore blocks, local semivariogram	129
4.9	S1.2, actual and average estimated error variance of 33 (100m*100m) ore blocks, one outlier removed	138
4.10	Combined regression analysis of four subareas, and mine method, for (100m*100m) ore blocks	142
4.11	Binomial statistics of actual errors/ estimated errors	155
5.1	Logarithmic estimation variance of (100m*25m) subblocks	161
5.2	Regression results of simple linear and lognormal kriging, (200m*50m) ore blocks	165

LIST OF SYMBOLS AND ABBREVIATIONS

Z	actual gold values
$\overline{Z}$	mean of actual gold values
Z^*	estimate of actual gold value Z
n	number of data
V^2	variance
b	additive constant beta for three-parameter log-normal model
Y	natural logarithm of gold value plus additive constant: $Y = \ln(Z+b)$
LV_b^2	logarithmic variance of three-parameter lognormal model.
LV^2	logarithmic variance of corresponding two - parameter lognormal model.
	both LV_b^2 and LV^2 have the same V^2.
V_e^2	error variance or estimation variance.
LV_e^2	logarithmic error or estimation variance
COV	covariance
LCOV	logarithmic covariance
G	semivariance
LG	Logarithmic semivariance
CoV	coefficient of variation = V^2 / Z^2
r	correlation coefficient
	semivariogram parameters:
C0	nugget effect
C1	sill of first structure
a1	range of first structure
C2	sill of second structure
a2	range of second structure (1/3 of practical range, if exponential model).

LIST OF SYMBOLS AND ABBREVIATIONS

Z	actual gold values
$\overline{Z}$	mean of actual gold values
Z^*	estimate of actual gold value Z
n	number of data
V^2	variance
b	additive constant beta for three parameter log-normal model
Y	natural logarithm of gold value plus additive constant: $Y = \ln(Z+b)$
LV_b^2	logarithmic variance of three-parameter lognormal model.
LV^2	logarithmic variance of corresponding two - parameter lognormal model.
	both LV_b^2 and LV^2 have the same V^2.
V_e^2	error variance or estimation variance.
LV_e^2	logarithmic error or estimation variance
COV	covariance
LCOV	logarithmic covariance
G	semivariance
LG	Logarithmic semivariance
CoV	coefficient of variation = V^2 / Z^2
r	correlation coefficient
	semivariogram parameters:
C0	nugget effect
C1	sill of first structure
a1	range of first structure
C2	sill of second structure
a2	range of second structure (1/3 of practical range, if exponential model).

Kriging methods:

SLK-GM simple lognormal kriging with population mean, either the global mean of the whole shaft area or the subarea mean after subdivision.

SLK-ST simple lognormal kriging with a local mean, calculated as mean of $(500m)^2$ area on the mined side of the ore block.

SLK-LT simple lognormal kriging with a local mean. A linear trend surface is fitted to the samples on the mined side of the ore block, and then extrapolated into the ore block to arrive at an estimate of a local mean.

OLK ordinary lognormal kriging.

SBK-GM simple linear kriging with population mean, either the global mean of the whole shaft area or the subarea mean after subdivision. A backtransformed semivariogram model is used.

SBK-ST simple linear kriging with a local mean, calculated as mean of $(500m)^2$ area on the mined side of the ore block. A back-transformed semivariogram model is used.

SBK-LT simple linear kriging with a local mean. A linear trend surface is fitted to the samples on the mined side of the ore block, and then extrapolated into the ore block to arrive at an estimate of a local mean. A backtransformed semivariogram model is used.

OBK ordinary linear kriging with a backtransformed semivariogram model.

UBK universal kriging (linear trend) with a back-transformed semivariogram model.

SHK-GM simple linear kriging with population mean, either the global mean of the whole shaft area or the subarea mean after subdivision. A Hawkins & Cressie semivariogram is used.

SHK-ST simple linear kriging with a local mean, calculated as mean of $(500m)^2$ area on the mined side of the ore block. A Hawkins & Cressie semivariogram is used.

SHK-LT simple linear kriging with a local mean. A linear trend surface is fitted to the samples on the mined side of the ore block, and then extrapolated into the ore block to arrive at an estimate of a local mean. A Hawkins & Cressie semivariogram is used.

OHK ordinary linear kriging with a Hawkins & Cressie semivariogram.

UHK universal kriging (linear trend) with a Hawkins & Cressie semivariogram.

Geological codes:

GB	Green Bar (shale)
PM	Rice Pebble Marker (arenite)
HW	Hanging Wall (quartzite)
RT	Carbon Leader reef - top conglomerate band
RI	Carbon Leader reef - internal waste (quartzite)
RS	Carbon Leader reef - shale layer
RB	Carbon Leader reef - bottom conglomerate band
RT	Carbon Leader reef - single conglomerate band
FW	Footwall (quartzite)

PREFACE

The Witwatersrand of South Africa contains the largest known gold deposits in the world. These have been mined now for more than a century; and it was these gold reefs that more than 30 years ago initiated the fundamental studies (Krige, 1951) that finally led to the development of the comprehensive theory of geostatistics (Matheron, 1963).

The theoretical basis of geostatistics is well established. In fact by comparing recent publications to the day to day work experienced by the author in a geostatistics department of a mining company, it is felt that the theoretical development at present is well ahead of its practical application.

This study is mainly based on geostatistical principles that have been known for 25 years or more. The investigation originated from a 'real world' problem, and the solution has been attempted by using proven geostatistical methods (e.g. Journel & Huijbregts, 1978).

Because the regionalized variable in question (gold) can be tied to geological features, the study tries to account for this fact.

Throughout the thesis the reader will find that it has been attempted to verify geostatistical assumptions by empirical investigations. It was found that, provided the basic assumptions (e.g. stationarity) are fulfilled, the comparison of theory with practice is acceptable.

1 INTRODUCTION

1.1 General

"Many new theoretical developments have been produced,..., but the basis of everyday's geostatistics, the one used in orebody modeling and mine planning, essentially remained the same. Comparing predictions and reality of course showed discrepancies, which could be reduced most of the time.

These discrepancies were reduced either by taking geology into account in better ways, or by checking more carefully that the basic statistical hypothesis were met. These two approaches, better respect of geology or better respect of statistical hypothesis are in fact equivalent and aim at the same single goal: a better orebody model." (David, 1988).

This quote borrowed from the introduction to M. David's new 'Handbook of Applied Advanced Geostatistical Ore Reserve Estimation' describes very well the main purpose of this study: In testing the implementation of geostatistical ore reserve estimation on an operating mine in the Carbon Leader reef, ensure that the orebody model is as optimal as possible in practice. In trying to do so, the improvements achieved by taking account of the geology are quantified.

The study is based on 'everyday's geostatistics', so most of the techniques used have been proven in practice for many years.

The geology of the area under study is known very well, and geological investigations were not the main aim of the thesis. The final geological input in the estimation procedure can be provided easily on a day to day basis, and does not require a departure from techniques already used in the mine practice. In this sense, not only 'everyday's geostatistics', but also 'everyday's geology' has been used. This combination should ensure the practical application of the results.

1.2 Outline

The ore estimation method currently applied at Western Deep Levels Gold Mine gives poor results in a certain area of the Carbon Leader reef. Recent investigations of this reef horizon indicate that the gold distribution pattern can be related to sedimentological features (Nami, 1983; Buck & Minter, 1985).

The influence geological control has on the effectiveness of geostatistical procedures, is well known, and it is generally accepted that geology is to be taken into account in geostatistical studies (e.g. Krige et. al.,1969; Magri, 1978; Rendu & Readdy, 1982; Rendu,1984; Benest & Winter, 1984).

Recent investigations of Witwatersrand gold reefs often stress the importance of the sedimentology for the ore evaluation (e.g. Magri, 1978; Verrezen, 1986; Reynolds & Stear, 1987), and suggest improved estimation by subdividing the orebody into sedimentologically homogeneous subareas. To date, however, this improvement has rarely been proved or even quantified in practice, at least not for the Carbon Leader reef. This investigation will do so.

By taking account of sedimentological parameters influencing the gold distribution, this study tests different geostatistical estimation methods to optimize the ore reserve estimation at Western Deep Levels. The longwall mining condition practiced at Western Deep Levels gold mine makes this difficult, as it requires the extrapolation of the sample values; and, like most estimation methods, kriging is basically an interpolation method.

As the data have to remain confidential, a constant factor is applied to all gold values, and only relative coordinates are revealed on the maps.

Because of the large amount of data and the complexity of the calculations involved in the analysis, a computer had to be used. The programs written by the author are described in Appendix 2.

1.3 Geographical and geological setting of the study area

Western Deep Levels Gold Mine is situated about 70 km west of Johannesburg in the Transvaal Province of South Africa. The mining district is known as the Carletonville Goldfield or West Wits Line and was discovered in 1930 (Krahmann,1936; see Figs. 1.1a & b).

At present mainly two reefs are mined for gold at Western Deep Levels gold mine: the Ventersdorp Contact Reef (VCR) and the Carbon Leader Reef (CL). These are tabular deposits of the Proterozoic Witwatersrand Sedimentary Basin.

There are many ideas and concepts as to the overall genetic origin of the Witwatersrand gold deposits, and these will not be discussed here in detail. The author finds a publication by Pretorius (Pretorius, 1981) very clear and concise for a general overview. The basic concept generally accepted for the origin of the gold bearing Witwatersrand conglomerates is that of sedimentary placer deposits.

The Carbon Leader reef is the objective of this study. It is one of the richest gold reefs mined in the Witwatersrand basin. The reef itself is a tabular conglomerate deposit with a maximum thickness of 3m (Buck

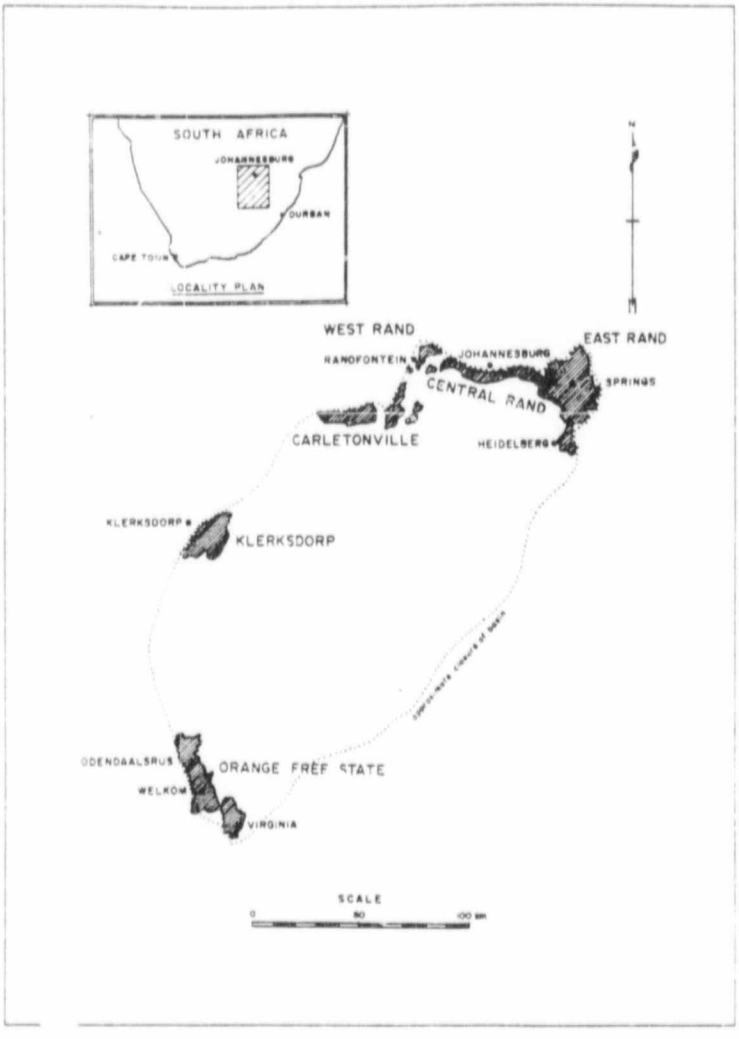


Figure 1.1a: Location of the Carletonville Goldfield in the Witwatersrand (after M. Lawlor, 1985).

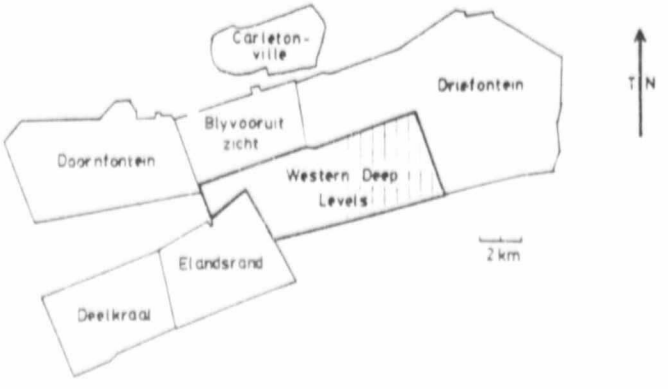


Figure 1.1b: Mining lease areas of the Carletonville Goldfield (modified, after M. Nami, 1983)

& Minter, 1985). Stratigraphically it occurs in the lower part of the Central Rand Group, about 60m above the Jeppestown Shales which top the West Rand Group (Buck & Minter, 1985). Uranium-lead dating suggests a minimum age of the Carbon Leader placer of 2700 million years (Armstrong et al., 1986).

The sediments are dipping south - southwest at an angle of 22 degrees. Figure 1.2 shows a geological section through the goldfield.

This study is conducted in the eastern part of Western Deep Levels in the No. 3 Shaft area (Fig. 1.1b).

The sub-outcrop in the north, and erosion by post Carbon Leader reef erosion channels in the east and west (de Kock,1964), form the margins of this reef on the sides. Todays available technology will limit mining towards the south, where with work proceeding at depths of 3700m below surface, Western Deep Levels has become the deepest mine in the world.

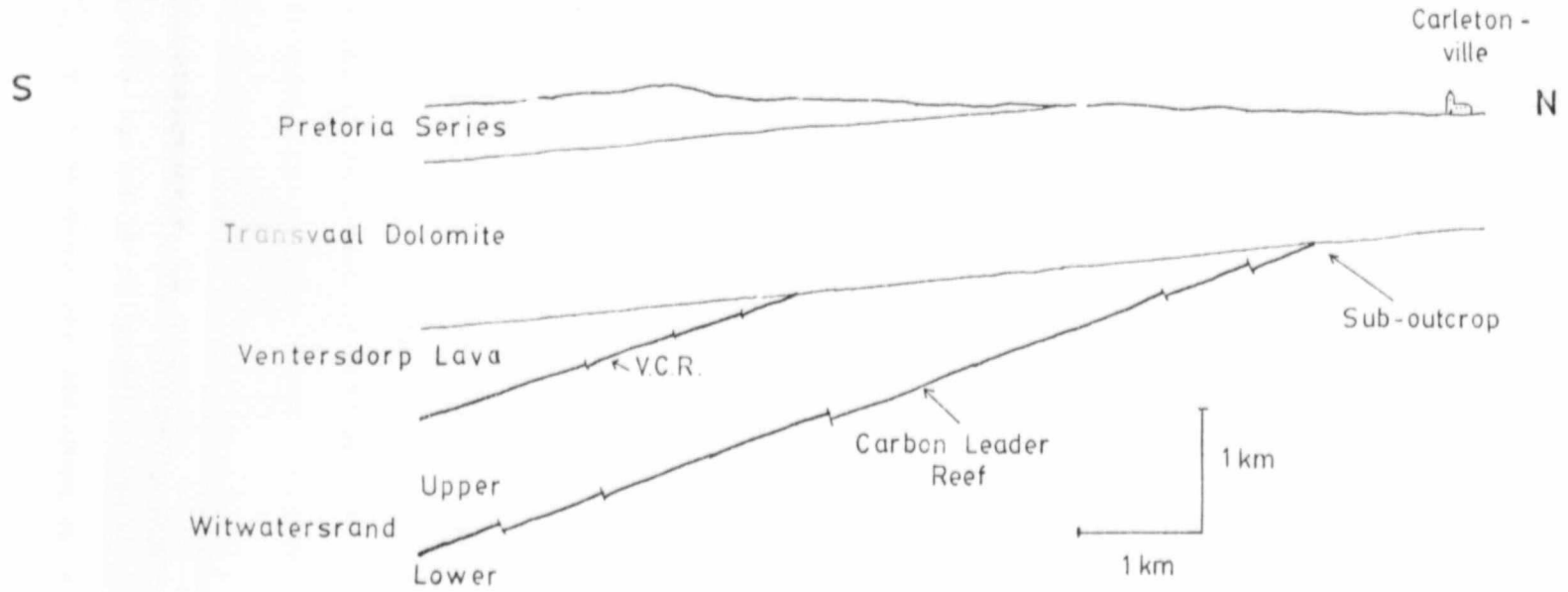


Figure 1.2: Geological north - south section through the Carletonville Goldfield(after T. Oberthür, 1883).

2 PREVIOUS INVESTIGATIONS IN THE RELATION OF GOLD DISTRIBUTION AND SEDIMENTOLOGY IN THE CARBON LEADER REEF

2.1 Description of Sedimentology

The Carbon Leader Formation is a fining upward cycle (the average grainsize in each layer reduces with the layer being higher up in the geological sequence, see Buck & Minter, 1985), starting at the base with the gold-bearing conglomerate band. This averages 0.1m in thickness, and rests on an angular unconformity (Buck & Minter, 1985). A carbon seam consisting of a maximum of 2 cm of columnar carbonaceous matter can be developed at the base of the conglomerate. This carbon seam is possibly the relic of primitive, Precambrian algal growth (Hallbauer, 1975). However, this carbon seam is not consistent in its lateral extent, and is not developed over large areas.

In north - south trending zones, this reef splits into several conglomerate bands, separated by intercalated quartzites. The cumulative thickness of up to 3m in these areas is achieved by downcutting into the underlying Footwall Quartzites (Buck & Minter, 1985).

This reef conglomerate is overlain transitionally by approximately 2m of dark green - gray Hangingwall Quartzites, which in turn are followed by a thin, well

sorted, coarse grained arenite band called Rice Pebble Marker. A laterally very consistent green shale to siltstone named Greenbar forms the top of the sequence.

The gold is found in the conglomerate unit. It occurs as detrital grains or as filaments in the columnar carbon seam and is distributed throughout the conglomerate, either detrital or intergrown with pyrite or gersdorffite. Most gold is concentrated in the basal carbon seam (Nami, 1983).

2.2 Interpretation of Sedimentology

Two sedimentological studies have been published with interpretations of the Carbon Leader, and investigations of the relationship of the gold distribution with sedimentological parameters, as mentioned in the outline (Nami, 1983; Buck & Minter, 1985).

While Buck and Minter (1985) investigated the whole goldfield on a regional scale, Nami did a very detailed study in a small area in the northwest of Blyvooruitzicht Gold Mine.

Buck and Minter (1985) interpreted the conglomerate unit as fluvial lag deposits of two adjacent palaeodrainage systems eroding an alluvial fan surface. The placer was formed through reworking and concentrating of fan material. The gold distribution pattern they found to be reflected in the cumulative conglomerate thickness, with high gold accumulations coinciding with channels.

Nami (1983) subdivided his study area into two subfacies: a subfacies A, also called Interchannel area, consisting of a single, thin sheet-like conglomerate; and a subfacies B or Channel area, which is characterised by two to three conglomerate bands separated by intercalated quartzites. While he also interpreted

multiple reef bands areas as palaeochannels, he assumes the single conglomerate band to be of sheetflood origin. These areas of thin placer development are interpreted as low energy - non active regions favourable for the existence of the primitive algae mass vegetation which later became the carbon seam. Because the gold most probably was transported in suspension (James, 1984), according to Nami most gold has been trapped by these algal mats. This resulted in a relative high uniform gold concentration in these areas, against a low and erratic gold concentration in the channel areas (Nami, 1983).

In conclusion it can be said that both researchers agree on the origin of the multiple conglomerate bands as channel-laid deposits. For the single conglomerate band the interpretations differ from shallow, probably migrating perennial streams to a sheetflood deposition.

It is generally expected that taking account of this geological information in the estimation process will improve the estimation in the Carbon Leader reef. However, no study has been published so far which actually quantifies this improvement.

3 SEDIMENTOLOGICAL STUDY

3.1 Method

It is the general underground practice to take a sedimentological log of the stope face at 5m intervals along the stope face. This practice is adhered to in order to ensure full compatibility with historical data. Taking logs at distinct locations also has the advantage that the exact position is known in north and east coordinates. Therefore the log positions can be digitized similar to borehole data.

The present practice is essential for the establishment of a computer-based geological data file. Another requirement for this data base is the coding of the information in a machine-readable form. This needs some standardization of the usual geological recording, as information like 'more pyrite in the bottom band than in the top band' has to be expressed as e.g.: pyrite content in bottom band: high, in top band: medium.

A log sheet ensuring this standard was developed at the Chamber of Mines of South Africa (pers. comm. M. Nami), and is shown in Figure 3.1. In addition, the stratigraphy is noted according to the code shown in Figure 3.2.

MINE: WDL WORKING PLACE: X: to be digitized

REEF: CL DATE: Y:

Strat.

SAMPLE NO.	REEF PROFILE	WIDTH	A	B	C	D	E	F	G	H
HW		12	02	05						
RT	1003	7	01	04	08	13	17	19	–	25
RI		8	02	05	–	13	–	–	–	–
RI	1002	21	01	04	07	13	17	18	–	26
RI		36	02	05	–	13	–	–	–	–
RB	1001	12	01	04	07	13	17	20	–	26
FW		14	–	05						

A – CONTACT NATURE

01 FLAT EROSIONAL
02 TRANSITIONAL
03 UNDULATING EROSIONAL

B – LITHOLOGY

04 CONGLOMERATE
05 QUARTZITE
06 SHALE

C – CONGLOMERATE PACKING

07 PEBBLE SUPPORTED (>70% PEBBLE)
08 MATRIX SUPPORTED (<70% PEBBLE)
09 SINGLE PEBBLE LAYER

D – SEDIMENTARY STRUCTURES

10 X-BEDDING TROUGH
11 X-BEDDING PLANAR
12 HORIZONTAL BEDDING
13 STRUCTURELESS (massive)
14 INCONSISTENT HORIZONS

E – MINERALIZATION TYPE OF PYRITE

15 MAINLY DETRITAL
16 MAINLY MUDBALL
17 MIXED PYRITE

F – PYRITE CONTENT

18 LOW ( )
19 MEDIUM ( )
20 HIGH ( )

G – CARBON

21 FLYSPEC
22 CARBON FILM OR SEAM

H – PEBBLE SIZE

23 > 8 cm
24 4-8 cm
25 2-4 cm
26 1-2 cm
27 0,5-1 cm
28 < 0,5 cm

Figure 3.1: Sedimentological Logging Sheet used for underground mapping (Chamber of Mines).

The coded information is stored in the data base.

A computer program (NIMROD, see Appendix 2.1) was developed by the author to allow fast automatic retrieval of the stored geological information.

GB: Green Bar
PM: Rice Pebble Marker
HW: Hangingwall Quartzite

RF: single conglomerate band
RT: top conglomerate band
RI: internal quartzite or conglomerate lense
RS: shale or siltstone
RB: bottom conglomerate band
RQ: basal quartzite

(basal conglomerate unit ('reef'))

FW: Footwall Quartzite

Figure 3.2: Stratigraphic code for different units.

During 72 underground shifts, all accessible stopes in the area under investigation were visited and sedimentological logs were taken at 401 positions.

Historical sedimentological information collected by mine personnel, is only available up to about 150m back from the workings, as it was not until two years before this study commenced that the relevance of sedimentology for the gold distribution was appreciated at Western Deep Levels.

So 1167 historical logs were coded and added to the data base.

Two different coordinate systems are used at the mine: north - east coordinates in a horizontal plane as on surface maps ,which are used for planning on the mine scale, and a north - east coordinate system in the plane of the reef, in which sampling and geological mapping is done. While in the strike direction of the reef (E-W) a distance remains the same when transferred to horizontal plane coordinates, the same distance in the dip direction (N-S) shortens and has to be multiplied by the cosine of the dip angle.

This shortening is maximal in the dip direction and zero at right angles to the dip direction, but has to be applied for all directions except in the strike direction of the reef plane.

There is no regional coordinate system for the reef plane; therefore, if localities are to be viewed on a mine scale, horizontal plane coordinates have to be used. Therefore the following study is based on the horizontal plane coordinate system. Because of the shallow dip, the distortion is minimal. Working in horizontal coordinates, however, requires dip correc-

tions for ore reserve estimates, as actual ore blocks in the plane of the reef are slightly larger than in the horizontal plane.

3.2 Practical limitations

Where the gold-bearing basal conglomerate unit averages 0.1m in width, as is the case in most areas, the stoping width is the minimum working height, and is approximately 1m.

About one third of the stope width is in the Footwall Quartzite, so that only the conglomerate unit and the lower part of the Hangingwall Quartzite are exposed. Information about the upper part of the Carbon Leader Formation can only be gained from drillholes.

In areas of multiple reef bands, it often happens that one band is left either in the hangingwall or footwall. Besides the loss of gold that is left behind, there is the problem of not having the full conglomerate unit exposed for mapping.

3.3 Description of the Carbon Leader reef in the study-area

Two main types of Carbon Leader reef are found in the area under investigation. The first type consists of a sequence of at least two, but up to four conglomerate layers, separated by quartzites, with a cumulative thickness including the quartzites of up to 1.7m. The second type is a rather thin, generally less than 0.25m thick conglomerate band which often shows reactivation surfaces, and in some areas overlies a carbon seam.

The first type always starts with a sharp, often undulating erosive, bottom contact to the Footwall Quartzite. Then follows a densely packed conglomerate layer of varying thickness, in places overlain by planar or trough crossbedded quartzites. This sequence is repeated up to three times, always starting with a sharp bottom contact. Only the bottom layer is laterally consistent over several adjacent stopes.

At some places, a sudden thickening of the bottom conglomerate band without downcutting into the Footwall Quartzite is observed. Here usually a thin (0.01m to max. 0.1m) shale or argillaceous quartzite is found overlying the intercalated quartzite and partly the conglomerate, as shown in Figure 3.3.

Thin shale layers, either consistent over tens of metres of stope faces, or with a lateral extension of only a few metres, can also overly either a conglomerate band or an internal quartzite.

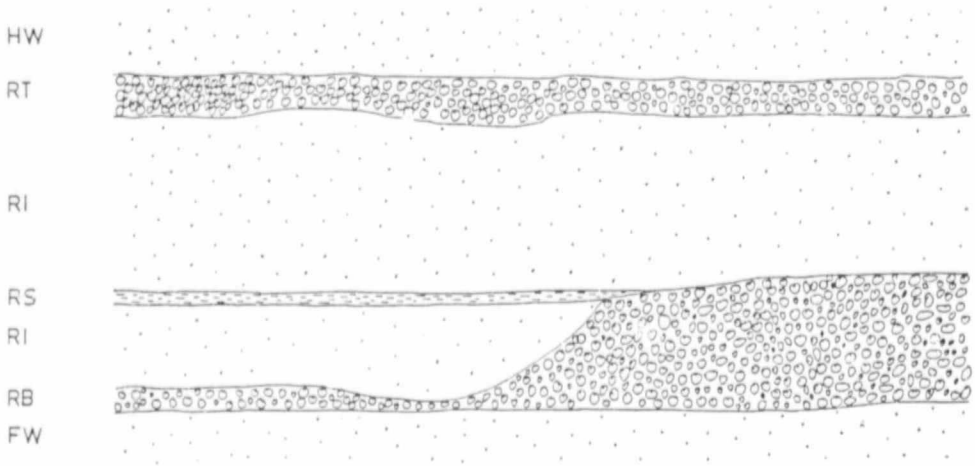


Figure 3.3: Sudden thickening of bottom conglomerate layer, and occurence of shale.

This whole sequence is then once again overlain by a laterally consistent conglomerate layer.

The base of the second reef type is also sharp. The reef itself consists of a rather uniform conglomerate layer. The thickness averages 0.1m and ranges in 95% of the measurements from a single pebble layer up to 0.25m of a mainly clast supported conglomerate, which at places shows reactivation surfaces. If a carbon

seam is developed, it usually rests immediately on the basal contact; carbon seams on reactivation surfaces are rarer and inconsistent.

In the transition zone of the two facies the top conglomerate band of the first reef type becomes the conglomerate layer of the second reef type, while the lower cycles of Reef Type 1 cut further down into the Footwall Quartzite (Fig. 3.4). It is therefore more accurate to call only the lower cycles Reef Type 1; while the top conglomerate band, being equivalent to Reef Type 2 should also be named so. Then areas where Reef Type 1 is overlain by Reef Type 2 (Subfacies 1) can be differentiated from areas exposing only Reef Type 2 (Subfacies 2).

This coincides with Nami's sub-facies B and sub-facies A (Nami, 1983).

The downcutting of Reef Type 1 into the Footwall Quartzite is generally very gradual. At the edges of Reef Type 1 zones against the Footwall Quartzite, the top conglomerate layer (Reef Type 2) rests with a sharp contact immediately on top of the Reef Type 1 bottom conglomerate, with an intercalated quartzite separating the two bands further towards the center of the Reef Type 1 area. Where the Reef Type 1 conglomerate does not reach the boundary of the Reef Type

1 zone to the Footwall Quartzite, the intercalated quartzite is found first, and this separates the Reef Type 2 conglomerate from the Footwall Quartzite. Towards the center this intercalated quartzite then overlies the Reef Type 1 conglomerate.

Figure 3.4 shows an idealized section through the two facies.

An analysis of the pebble sizes measured in 131 samples shows that this is no reliable indicator of the different reef types. The average diameter of the 10 largest pebbles per sample is 1.7cm and does not vary significantly over the study area. This was found by Nami in his investigation as well; he also concluded that the composition of the conglomerate components shows no significant variation (Nami,1983).

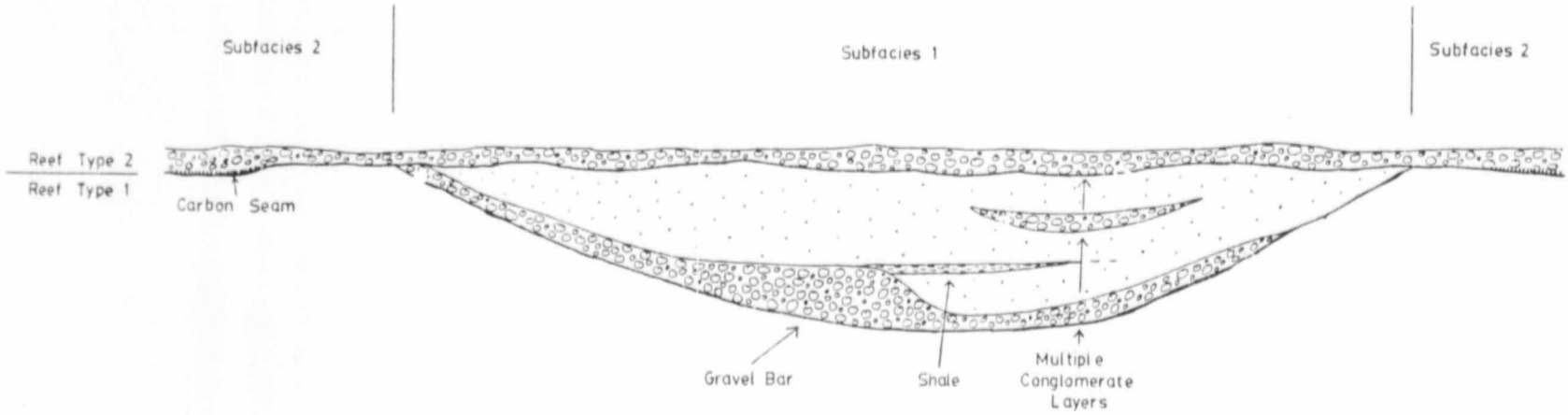


Figure 3.4: Idealized sedimentological section through the Conglomerate Unit. Sections exposing Reef Type 2 only can be separated from sections showing both reef types; thus allowing the subdivision of the Conglomerate Unit into two subfacies in plan view.

3.4 Classification of sedimentary characteristics

In general, the cumulative thickness of the basal conglomerate unit is a sufficient criterion to distinguish between the two reef types. While Subfacies 2 can hardly be misinterpreted, Subfacies 1 can present a problem if only the bottom conglomerate band is exposed and the top band is left in the hangingwall. This can be mistaken for the single conglomerate band type reef. Then the different features of the reef types as described under 3.3 can assist in the interpretation. The following Table lists the immediately recognizable characteristics of the two reef types.

Table 3.1: Reef Type characteristics

characteristics	reef type 1	reef type 2
conglomerate thickness	up to 1.00m, changes might be abrupt(gravel bars)	less than 0.25m* gradual changes
erosional contact	flat or undulating	flat
shale layers	often present	absent
No.of conglomerate bands	2 to 4 (if whole unit exposed)	1

These characteristics are valuable for underground mapping in areas which are problematic because of conglomerate bands possibly not exposed.

* See explanation, 1st paragraph page 18.

3.5 Interpretation of Sedimentology

The two different reef types were probably formed in different environments.

Reef Type 1 is thought of as being deposited in a fluvial environment.

The vertical succession of several conglomerate bands, each with an erosional base, and intercalated quartzites, are interpreted as fluvial sediments, deposited in several events on top of each other (Reineck & Singh, 1980).

The sudden thickening of a bottom conglomerate layer that occurs in this reef type (as illustrated in Figure 3.3), is interpreted as a gravel bar (Reineck & Singh, 1980, p. 257ff). With decreasing competence of the water flow, these gravel bars are formed first, and direct the water flow in the channel. Continuous further decrease causes the gravel bars to fall dry, and makes the remaining parts of the channel suitable for the deposition of sand. Eventually the water flow will become stagnant, and the clay is deposited between the gravel bars.

Thin intercalated shale layers occurring without gravel bars are thought of as being formed in a similar way.

The deposition of clay is confined to stagnant water. This will collect in low lying areas. These shale layers are therefore characteristic of the Subfacies 1 channels, which eroded below the palaeosurface.

The extension of the oblong areas in which Reef Type 1 occurs, in a north - south direction, also fits into the general pattern of a palaeodrainage system flowing from the hinterland in the north to the Witwatersrand Basin in the south (de Kock, 1964).

Reef Type 2 does not show any of these characteristics. It is a thin, laterally consistent, sheetlike conglomerate band, covering areas in which Reef Type 1 was deposited as well as areas where this is absent. The basal contact is planar. Shale layers are absent. No downdip decrease in pebble size is displayed (Nami, 1983).

All this points towards a uniform depositional process.

The genesis of the Carbon Leader is visualized as follows: due to tectonic uplift in the hinterland, a fluvial fan system started discharging sediment over the plain formed by the Footwall Quartzites. The first event was erosive downcutting in the Footwall Quartzites. These channels were then filled, firstly with conglomerates, and in later stages with sand, and

The deposition of clay is confined to stagnant water. This will collect in low lying areas. These shale layers are therefore characteristic of the Subfacies 1 channels, which eroded below the palaeosurface.

The extension of the oblong areas in which Reef Type 1 occurs, in a north - south direction, also fits into the general pattern of a palaeodrainage system flowing from the hinterland in the north to the Witwatersrand Basin in the south (de Kock, 1964).

Reef Type 2 does not show any of these characteristics. It is a thin, laterally consistent, sheetlike conglomerate band, covering areas in which Reef Type 1 was deposited as well as areas where this is absent. The basal contact is planar. Shale layers are absent. No downdip decrease in pebble size is displayed (Nami, 1983).

All this points towards a uniform depositional process.

The genesis of the Carbon Leader is visualized as follows: due to tectonic uplift in the hinterland, a fluvial fan system started discharging sediment over the plain formed by the Footwall Quartzites. The first event was erosive downcutting in the Footwall Quartzites. These channels were then filled, firstly with conglomerates, and in later stages with sand, and

eventually clay. Several phases of deposition took place, with the main water flow always confined to the channels. Reef Type 1 was formed in this manner.
During the deposition of Reef Type 1, the areas between the channels stayed virtually free of sediment. They formed favourable conditions for the primitive algal growth, that later became the carbon seam. During high flood stages, water and gold particles (that are mainly transported in suspension (James, 1984)), reached these areas, and the gold particles were deposited here because of the changed flow conditions.

This resulted in a consistently high gold content in the areas between the channels, while the channels themselves have only an erratic, and generally low gold content.

This is the situation before the deposition of the Reef Type 2 conglomerate, as described by Nami (Nami, 1983).

New research in other carbon-seam type gold reefs on the Witwatersrand (Verrezen, 1987) make a different genesis for Reef Type 2 more probable than the sheetflood deposition originally assumed by Nami (Nami, 1983). Prolonged discussions with Nami and Verrezen (pers. comm.) led to the interpretation of Reef Type 2 of the Carbon Leader reef as the basal conglomerate of a marine transgression over the fluvial plain, on which

Reef Type 1 was formed. The wide lateral extension and continuity of the Reef Type 2 conglomerate band suggests a marine environment (Clifton, 1973).
The marine transgression was caused by a downlift of the floodplain. Hangingwall Quartzite, and Greenbar shales were deposits of the marine environment, with the Rice Pebble Marker at the base of the Greenbar, possibly being a product of an intermediate uplift period before the deposition of the Greenbar shales.

Uplifting after the Greenbar deposition caused this to fall dry, and later to become covered with sediments deposited in a fluvial environment.

Figure 3.5 shows a schematic block diagram illustrating this sedimentological model. It is very much in agreement with the general model given by Pretorius who describes this reef type as 'transgressive placer' (Pretorius, 1981).

As this model accomodates most of the sedimentological properties of the Carbon Leader, it is chosen as the geological basis of the geostatistical study.

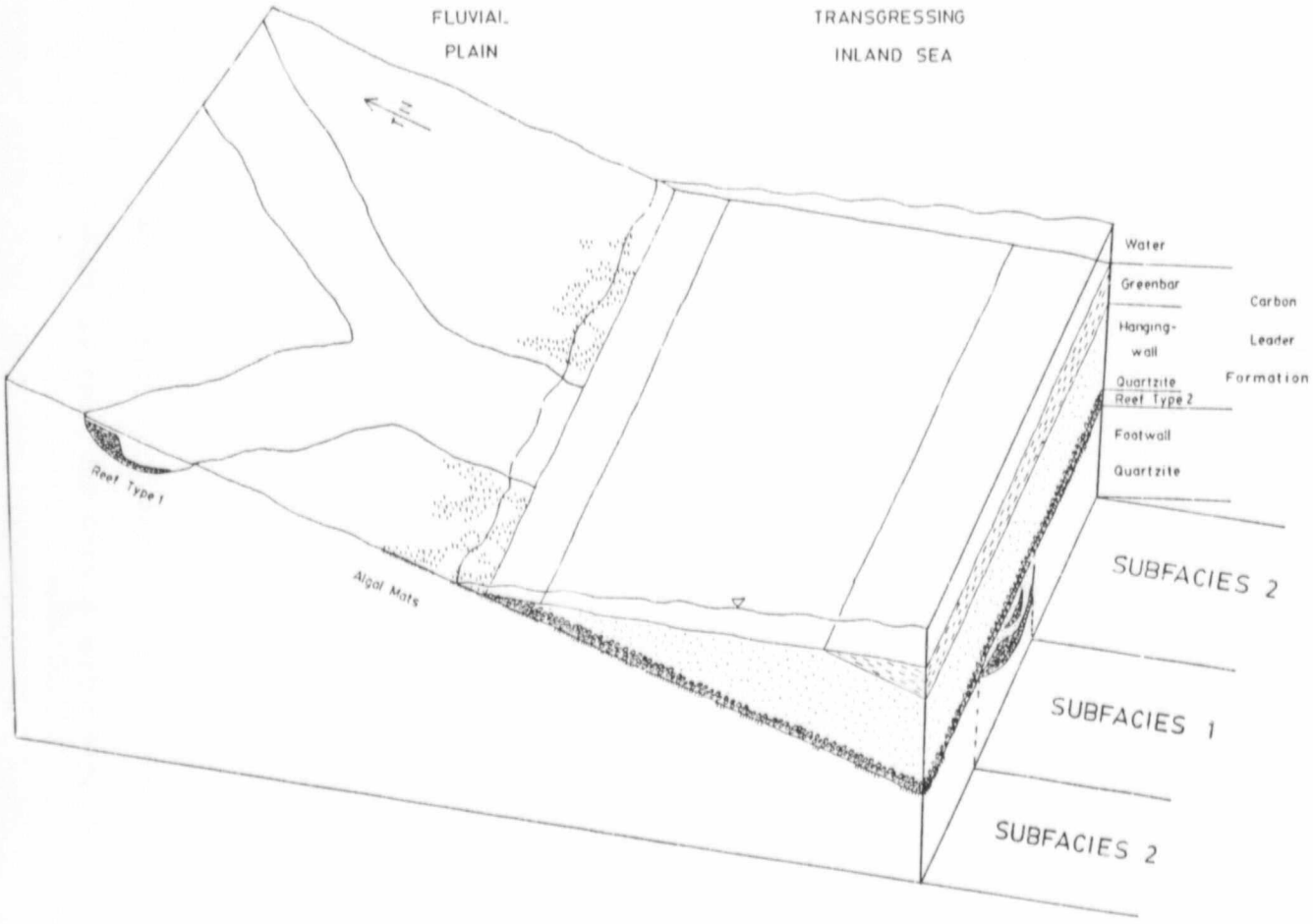


Fig. 3.5: Schematic, vertically strongly exaggerated block diagram of depositional model. Influx of sediment and heavy minerals by fluvial fan system into transgressive inland sea. Local reworking and winnowing in beach zone concentrates pebbles and heavy minerals. Transgression creates sheetlike conglomerate unit covering fluvial channels (Subfacies 1 in plan view) and Footwall Quartzite alike (Subfacies 2). Color scheme according to standard of AAC.

3.6 Facies Distribution in Study Area

3.6.1 Comparison of Geological Data with Sampling Data

In order to draw a map of the subfacies distribution in the No. 3 Shaft area, it is necessary to rely on the channel width as recorded during routine chip sampling as for most of the mined out area no other information is available (see chap. 3.1). This channel width is ideally the cumulative thickness of the conglomerate unit including the intercalated quartzites, but can be misleading in multiple conglomerate band areas, where for example the top conglomerate band is not exposed. Such a case is illustrated in Figure 3.6.

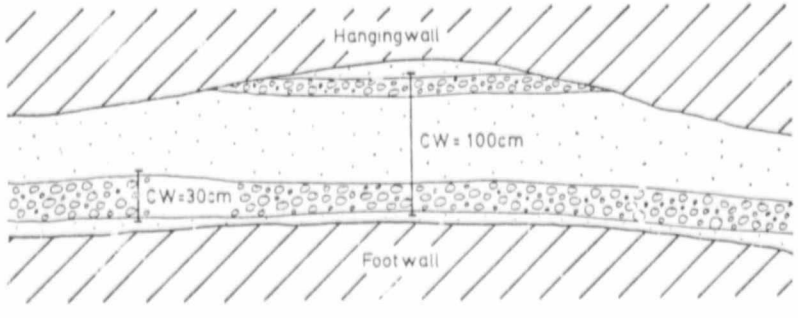


Figure 3.6: Influence of reef in hangingwall on channel width as recorded during assay sampling.

As can be seen, severe underestimation of the true channel width may occur if the conglomerate unit is not fully exposed.

These channel width data are compared with the true channel width resulting from sedimentological mapping in recently mined areas where both types of data are available.

Both data sets are regularized in $(25m)^2$ blocks. From each sample width 4cm are substracted, as samplers are advised to include 2cm of hangingwall and footwall into their samples. Only those geological data which cover the whole reef section between footwall and hangingwall are included in the analysis.

In Subfacies 1, 152 blocks of $(25m)^2$ each were found, for which geological and sampling data are available, and 218 of such blocks for Subfacies 2. Table 3.2 shows the result of a correlation analysis of the variable channel width for these two data sets as well as for the combined position for all blocks.

Although the overall correlation coefficient of .77 indicates a reasonable correlation of the data sets, the discrepancy increases if the subfacies are analysed individually. For Subfacies 1, the sample data underestimate the true channel width on average by 28%. This

is to be expected because of the not fully exposed conglomerate unit. For Subfacies 2 the sample data overestimate the true channel width by 29% on average, probably due to the tendency of the samplers to also sample pebbly Hangingwall Quartzite as well as footwall pebble bands.

Table 3.2: Correlation of channel width as recorded by geologists (CWgeol) and samplers (CWsamp).

	CWgeol		CWsamp			
	mean (cm)	V^2 (cm^2)	mean (cm)	V^2 (cm^2)	r	n
Subfacies 1	54.5	21.5	39.5	17.8	.56	152
Subfacies 2	11 3	5.8	14.6	9.4	.31	218
Combined	29.0	25.7	24.8	18.2	.77	370

r: correlation coefficient n: number of samples

In Figure 3.7, this is shown graphically. The two data sets are plotted against each other for the combined data set of Table 3.2 .

The dashed horizontal line represents the boundary between the two subfacies, and the solid sloping line is the line X=Y. The true channel widths of blocks plotting on this line are exactly estimated through the sample channel width. Points above the line X=Y represent blocks for which the samplers underestimate and points below blocks for which they overestimate the

true channel width. For Subfacies 1 - above the dashed line - most points plot above the line X=Y, thus showing the general underestimation of the true channel width by the samplers in this subfacies.

Below the horizontal line, the majority of the points falls under the line X=Y, showing that the true channel width is on average overestimated for Subfacies 2.

A linear regression analysis of the true channel width on the channel width as recorded during routine sampling gives the regression formula:

$$CWgeol = 2.18cm + 1.08 * CWsamp$$

with a standard error of 16.6cm.

In general it is concluded that channel width data are reliable indicators of the subfacies distribution. However, in localized areas it can be misleading. As Figure 3.7 shows, in an extreme case a block with a true channel width of about 8cm was sampled over a width of 64cm! The other extreme is where blocks of 65cm true channel width give a sample channel width of less than 5cm. Therefore not too much weight should be given to isolated patches of what appears to be one subfacies within the general area of the other sub-

facies, as that is well within the accuracy of a sub-facies map based on channel width data as recorded during routine sampling.

Author Braun Rolf
Name of thesis A Study To Optimize Ore Evaluation At Western Deep Levels Gold Mine, Witwatersrand, By Using Geostatistics And Geological Subdivision. 1988

PUBLISHER:
University of the Witwatersrand, Johannesburg
©2013

LEGAL NOTICES:

Copyright Notice: All materials on the University of the Witwatersrand, Johannesburg Library website are protected by South African copyright law and may not be distributed, transmitted, displayed, or otherwise published in any format, without the prior written permission of the copyright owner.

Disclaimer and Terms of Use: Provided that you maintain all copyright and other notices contained therein, you may download material (one machine readable copy and one print copy per page) for your personal and/or educational non-commercial use only.

The University of the Witwatersrand, Johannesburg, is not responsible for any errors or omissions and excludes any and all liability for any errors in or omissions from the information on the Library website.